Published by Institute of Physics Publishing for SISSA

Received: *July 11, 2007*
Accepted: *August 26, 2007*
Published: *September 14, 2007*

Absorption lengths in the holographic plasma

Irene Amado,[a] **Carlos Hoyos,**[b] **Karl Landsteiner**[a] **and Sergio Montero**[a]

[a] *Instituto de Física Teórica, C-XVI Universidad Autónoma de Madrid, E-28049 Madrid, Spain*
[b] *Department of Physics, Swansea University, Swansea, SA2 8PP, U.K.*
E-mail: Irene.Amado@uam.es, Karl.Landsteiner@uam.es, Sergio.Montero@uam.es, C.H.Badajoz@swansea.ac.uk

Abstract: We consider the effect of a periodic perturbation with frequency ω on the holographic $\mathcal{N} = 4$ plasma represented by the planar AdS black hole. The response of the system is given by exponentially decaying waves. The corresponding complex wave numbers can be found by solving wave equations in the AdS black hole background with infalling boundary conditions on the horizon in an analogous way as in the calculation of quasinormal modes. The complex momentum eigenvalues have an interpretation as poles of the retarded Green's functions, where the inverse of the imaginary part gives an absorption length λ. At zero frequency we obtain the screening length for a static field. These are directly related to the glueball masses in the dimensionally reduced theory. We also point out that the longest screening length corresponds to an operator with non-vanishing R-charge and thus does not have an interpretation as a QCD_3 glueball.

Keywords: AdS-CFT Correspondence, Gauge-gravity correspondence.

JHEP09(2007)057

Contents

1. Introduction

The AdS/CFT correspondence is a concrete realization of the idea that the large-N limit of non-Abelian gauge theories can be described by a dual string theory [1]. In the large 't Hooft coupling regime the dual theory admits a description in terms of gravitational fields over a weakly curved background. More precisely the AdS/CFT correspondence proposes an exact duality between $\mathcal{N}=4$ super Yang-Mills in four dimensions and type IIB superstrings in $\mathrm{AdS}_5 \times \mathrm{S}^5$. This theory is conformal, but at finite temperature conformal symmetry is broken and the theory is in a deconfining (or plasma) phase. The dual description corresponds to a black hole geometry with flat horizon [2].

Heavy-ion collisions at RHIC [3] and lattice simulations [4] indicate that QCD actually stays strongly coupled above the deconfinement transition up to temperatures $T \sim 2T_c$. Therefore, it is of great interest to develop non-perturbative tools that can describe the properties of the strongly coupled plasma. Lattice simulations are good to describe thermodynamical properties, but out-of-equilibrium processes are much harder to analyze. In this context, the AdS/CFT correspondence could provide a better framework to derive some plasma properties using analytic methods. Although $\mathcal{N}=4$ is far from QCD, some qualitative properties of the plasma seem to be quite similar, and AdS/CFT computations

JHEP09(2007)057

of the shear viscosity [5], the energy loss rate of a heavy quark [6] or the jet quenching parameter using light-like Wilson loops [7] show good agreement with experimental data.

Many of the properties of the plasma can be studied using linear response theory. In this approximation, small perturbations that do not change significantly the state of the plasma are introduced. The system then tries to restore thermal equilibrium. That involves *dissipation* if the perturbations are localized in time or *absorption* if they are localized in space.[1] We would like to address the latter in this work. The absorption is directly related to spatial correlations in the equilibrium state. At high temperatures the system is in a very disordered phase, so measures made in different parts of the plasma give uncorrelated results. For the same reason, a small perturbation cannot travel too far in the plasma before being washed out by thermal fluctuations. How far this can be depends on the details of the plasma, but in general we expect that the characteristic absorption lengths decrease as the temperature increases.

In the gravity dual picture the absorptive properties of the plasma rely on the presence of a horizon. Small classical perturbations end up falling into the horizon, either after a finite time or after travelling a finite distance.[2] The first is described by complex values for the eigenfrequency, the quasinormal modes, and the second by complex momentum values. Both are intimately related, they correspond to solutions of the linearized equations of motion. They also satisfy the same boundary conditions, Dirichlet at the AdS boundary[3] and infalling at the horizon. The difference is that quasinormal modes decay exponentially in time while complex momenta describe the decay along the direction of propagation. The choice of boundary conditions restricts the possible values of complex frequency or momentum to a discrete set. In the dual gauge theory we can interpret them as inverse relaxation times τ or inverse absorption lengths λ of the plasma. The relaxation time depends on the (real-valued) wave number k whereas the absorption length depends on the (real-valued) frequency ω, i.e. $\lambda = \lambda(\omega)$. In the gravity theory we therefore fix a frequency, impose infalling boundary conditions on the horizon and search then for a solution of the boundary condition at infinity in the complexified momentum plane. In this way we can compute the frequency dependence of the absorption lengths.

Quasinormal modes have been much studied in the context of black holes in flat spacetime (see [9] for a review) and in the AdS/CFT correspondence [10 – 13, 8, 14, 15]. Complex momenta have been studied for horizons of compact spatial geometry, where they correspond to Regge poles [16] of the black hole S-matrix. In the AdS/CFT correspondence, the zero frequency limit of complex momenta gives the glueball masses of QCD_3, as computed in refs. [17 – 19]. While this work was in progress the interpretation of glueball masses as correlation lengths was also emphasized in [20].

The content of the paper is the following. In section 2 we explain in detail the relation between complex momenta and absorption lengths. We show that they arise as the poles of the retarded Green's function and give an argument based on stability considerations

[1] There can also be diffusion effects if conserved charges are involved.

[2] In AdS space the curvature acts effectively as a box, so they cannot escape to infinity.

[3] Actually, the condition is that they should be normalizable modes, so in the gauge theory they correspond to states and not to the insertion of sources or couplings (c.f. [8]).

JHEP09(2007)057

showing that the poles have to lie in the first and third quadrants of the complex momentum plane. In section 3, we compute the frequency dependence of the largest correlation lengths for scalar operators of conformal dimension $\Delta = 4$, global currents, and the transverse and shear channels of the stress-energy tensor, respectively. We also show the relation with QCD_3 glueball masses. The paper ends with a summary of our results and some outlook to future possible investigations in section 4. In appendix A we comment on the form of the effective potentials that arise in rewriting the wave equations on AdS in the form of a Schrödinger equation and in appendix B we show how to avoid the "false frequencies" that arise in the numerical algorithm based on the Heun equation [13].

2. Absorption lengths in AdS/CFT

In ref. [22] the authors gave a prescription to compute retarded two-point Green's functions in the context of the AdS/CFT correspondence with Lorentzian signature. It was emphasized that retarded propagators correspond to imposing an *infalling* boundary condition at the horizon for the fields on the gravity side. On the other hand, infalling boundary conditions are also the constitutive ingredient for the calculation of the quasinormal frequencies of black holes in anti de Sitter space [10].[4] The authors of [11] observed that the quasinormal frequencies of BTZ black holes coincide with the poles of the retarded two-point functions in the dual two dimensional conformal field theory. In [13, 8] it was shown that this observation extends generally to the Lorentzian AdS/CFT correspondence, i.e. quasinormal frequencies in AdS can be interpreted as the poles of retarded Green's functions in the dual field theory.

Let us remember the interpretation of the poles of the retarded Green's function $G_{\rm R}$. The response in the field ϕ of the system under consideration is obtained by the convolution of the perturbation represented by the source $j(t, \mathbf{x})$ with the retarded Green's function

$$\phi(t, \mathbf{x}) := -\int \mathrm{d}\tau \, \mathrm{d}\boldsymbol{\xi} \; G_{\rm R}(t - \tau, \mathbf{x} - \boldsymbol{\xi}) \, j(\tau, \boldsymbol{\xi}) \; . \tag{2.1}$$

If one chooses a perturbation localized in time, figuratively speaking one "hits" the plasma once at time $t = 0$, the perturbation is given by $j(t, \mathbf{x}) = \delta(t) \exp(i\mathbf{q}\mathbf{x})$.[5] Considering the Fourier transform of the retarded propagator and performing τ and $\boldsymbol{\xi}$ integrations one arrives at

$$\phi(t, \mathbf{x}) = -\frac{\mathrm{e}^{i\mathbf{q}\mathbf{x}}}{2\pi} \int \mathrm{d}\nu \; \widetilde{G}_{\rm R}(\nu, \mathbf{q}) \, \mathrm{e}^{-i\nu t} \; . \tag{2.2}$$

One can now make the analytical continuation to the complex ν-plane and use Cauchy's theorem. For $t > 0$ we form a closed contour with a semicircle at infinity on the lower-half ν-plane, whereas for $t < 0$ we would close it in the upper-half ν-plane. One obtains

$$\phi(t, \mathbf{x}) = i \, \mathrm{sign}(t) \, \mathrm{e}^{i\mathbf{q}\mathbf{x}} \sum_{\nu_n : \mathrm{poles}} \mathrm{e}^{-i\nu_n t} \; \mathrm{Res} \, \widetilde{G}_{\rm R}(\nu, \mathbf{q}) \Big|_{\nu = \nu_n} \; , \tag{2.3}$$

[4] For a more general review of quasinormal modes see [9].

[5] The x-dependence is that of a plane wave; however a general dependence can be constructed by superpositions of plane waves.

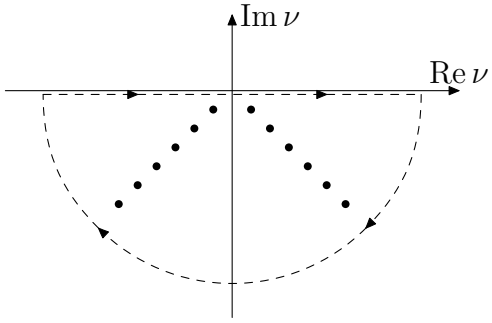

Figure 1: The relevant integration contour for the poles in the ν-plane. All the poles are in the lower-half plane, corresponding to the interpretation of quasinormal modes as the poles of a *retarded* Green's function.

At this point we assume that the retarded Green's function is analytic in the upper half of the frequency plane and that its only singularities are single poles in the lower half plane. This is indeed the analytic structure that appears in the Lorentzian AdS/CFT correspondence at finite temperature [8]. In general, the analytic structure of retarded two-point functions is of course more complicated and involves also branch cuts. The authors of [21] computed the retarded two-point function of tr (F^2) at weak coupling and found a tower of branch cuts with branch points located at $\omega \pm q = -i4\pi nT$. In this paper we will only consider the strict large N and strong coupling limit. Therefore, the response of the system to a perturbation localized in time is determined by the sum over the residues of $\widetilde{G}_{\rm R}$ at the poles. In the holographic gauge theory these poles are *precisely* the quasinormal frequencies of the perturbation on AdS space subject to the *infalling* boundary condition.

Instabilities, i.e. exponentially growing modes, appear as quasinormal frequencies with positive imaginary part. This is consistent with the interpretation as retarded Green's function, where singularities in the upper half plane would correspond to tachyonic modes travelling backwards in time. A typical arrangement of quasinormal frequencies as they appear in the analysis of small perturbations of asymptotically AdS black hole spacetimes is depicted in figure 1.

Let us choose now another kind of perturbation. This time we will pick a periodic perturbation localized in space, i.e. we switch the roles of time and one space coordinate and assume a source of the form $j(t, \mathbf{x}) = \delta(x) \exp[-i(\omega t - \mathbf{k}_\perp \mathbf{x}_\perp)]$. We compute the effect of such a perturbation again in linear response theory. Doing the Fourier transform of the retarded propagator and performing $\boldsymbol{\xi}_\perp$ and τ integrations one finds

$$\phi(t, \mathbf{x}) = -\frac{1}{(2\pi)} \, \mathrm{e}^{-i(\omega t - \mathbf{k}_\perp \mathbf{x}_\perp)} \int \mathrm{d}q \; \widetilde{G}_{\rm R}(\omega, \mathbf{k}_\perp, q) \; \mathrm{e}^{iqx} \,, \tag{2.4}$$

This is the response of the system to a periodic perturbation with frequency ω that is localized in the x-direction and has the form of a plane wave in the perpendicular directions $\mathbf{x}_\perp$. We have assumed that the perturbation has started far in the past such that all transient oscillations have already vanished and the system has reached a stationary state. In the following we will also assume that the perturbation is not further modulated in the

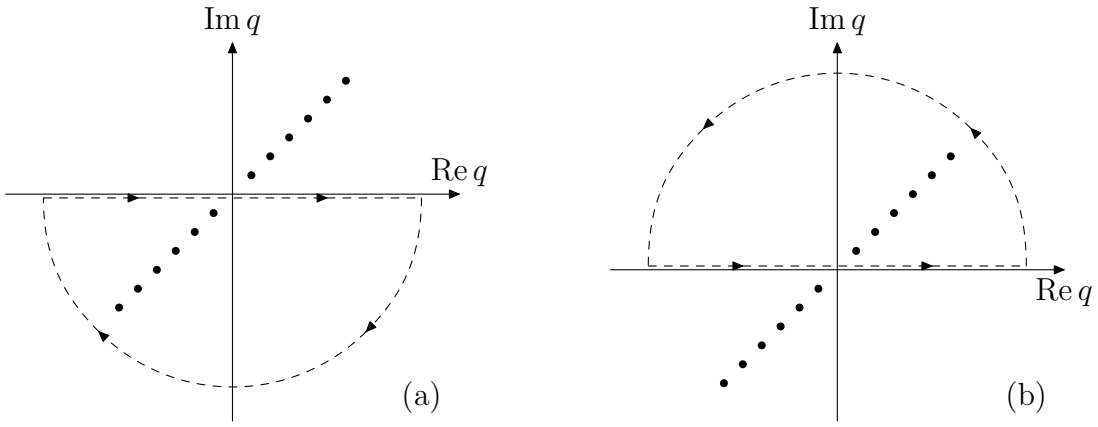

Figure 2: The relevant integration contours for the poles in the complexified momentum-plane. Figure (a) shows the contour for $x < 0$, and figure (b) shows the contour for $x > 0$. In order to obtain exponentially decaying waves travelling away from the origin of the perturbation it is necessary that the poles lie in the 1st and 3rd quadrants.

$\mathbf{x}_\perp$-directions, i.e. we set $\mathbf{k}_\perp = 0$. Now one can use again Cauchy's theorem, closing in the upper or lower-half planes for $x > 0$ and $x < 0$, respectively. The result is

$$\phi(t,x) = -i\ \mathrm{sign}(x)\, \mathrm{e}^{-i\omega t} \sum_{q_n:\mathrm{poles}} \mathrm{e}^{iq_n x}\ \mathrm{Res}\, \widetilde{G}_{\mathrm{R}}(\omega,q)\Big|_{q=q_n}\,, \tag{2.5}$$

Again we have assumed that the only singularities of $G_{\mathrm{R}}(\omega,\mathbf{q})$ are poles in the complexified momentum plane. By symmetry considerations ($x \to -x$) it is clear that if $q = q_n = q_n^R + iq_n^I$ is a pole then also $q = -q_n$ has to be a pole. We would like the poles in the upper-half to lie in the first quadrant and those in the lower-half in the third quadrant. With such and arrangement of poles the perturbation is creating damped waves moving to the right for $x > 0$ and to the left for $x < 0$. The waves propagate away from the origin of the perturbation at $x = 0$ and are exponentially decaying with the distance from the perturbation. In subsection 2.1 we prove that for the holographic retarded two-point functions the poles do indeed fall into the first and third quadrants of the complex momentum plane. A typical setup with the corresponding integration contours is depicted in figure 2. The imaginary part of the complex wave number can be interpreted as the inverse of an *absorption length*. For a given complex momentum pole q_n the right-moving wave has the form $\mathrm{e}^{-i(\omega t - q_n^R x)}\, \mathrm{e}^{-q_n^I x}$. The amplitude of the wave has decayed to a factor of $1/e$ at a distance of $\lambda_n = 1/q_n^I$.

In the following we will be interested in computing these absorption lengths and their frequency dependence in the holographic dual of the $\mathcal{N}=4$ supersymmetric gauge theory in the plasma phase. We will do this for different kinds of perturbations corresponding to certain gauge-invariant operators. In the gravity side we have to solve wave equations with purely infalling boundary conditions at the horizon just as in the calculation of quasinormal modes. At the boundary of AdS we have to specify the same boundary conditions that have been described in refs. [13, 8] for the quasinormal modes. The imaginary part of these

JHEP09(2007)057

complex momentum wave numbers give absorption lengths characteristic of the black hole. After having traveled a distance λ_n a part of the wave has fallen into the black hole such that the amplitude is diminished by a factor of e^{-1}. In the gauge theory dual the inverse of the imaginary part of the momenta can be seen as the absorption lengths for perturbations of the plasma by sources corresponding to gauge-invariant operators.

Thus, we see that in both cases — relaxation times and absorption lengths — the gravity waves are subject to the infalling condition at the horizon. The question is simply which parameter of the retarded Green's function is analytically continued to complex values, either the frequency or the momentum. To compute these complex momentum wave numbers one can therefore follow the same strategy that is used for the calculation of quasinormal frequencies, but fixing the frequency ω to be real-valued instead of the momentum q.

This switch of roles is particularly clear in the case of the AdS_3/CFT_2 correspondence, where the exact retarded Green's functions can be calculated in both sides and seen to match [11]. Let us consider the case of a field with conformal dimension $\Delta = 2$. Then the retarded two-point function is

$$G_{\mathrm{R}}^{(2\mathrm{d})}(\omega, q) = \frac{\omega^2 - q^2}{4\pi^2} \left[\psi\left(1 - i\,\frac{\omega - q}{4\pi T}\right) + \psi\left(1 - i\,\frac{\omega + q}{4\pi T}\right) \right] . \tag{2.6}$$

The poles of the ψ function determine the quasinormal frequencies $\omega_n = \pm q - i4\pi T(n+1)$. For each quasinormal mode the dispersion relation $\omega_n = \omega_n(q)$ is linear. Because of this linearity the poles can also be interpreted in a different way by writing

$$q_n = \pm[\omega + i4\pi T(n+1)]\,, \quad n \in \mathbb{N}\,, \tag{2.7}$$

where we see explicitly that the complex momentum modes lie in the first and third quadrants for the right- and left-movers respectively.

In higher dimensions the dispersion relations for the quasinormal frequencies are not linear and can be computed only numerically. At zero momentum, the position of large frequencies in the complex momentum plane has been estimated using semiclassical methods [24], it would be interesting to extend those analysis to non-zero momentum. Since the dispersion relation for the quasinormal modes is known only numerically we also have to resort to numerical methods to find the complex wave numbers and absorption lengths. The only exception is given by the hydrodynamic modes that appear for small frequency and wave numbers [25, 26]. We will see that our numerical results are in agreement with the analytic dispersion relations of the hydrodynamic modes.

2.1 Stability analysis

We will now perform a stability analysis analogous to the one for quasinormal modes in [10]. We will see that the complex momentum wave numbers indeed lie in the first and third quadrants of the complex q-plane for positive frequencies. Note that a pole in the second or fourth quadrant would allow to construct outgoing waves that are exponentially growing with the distance from the perturbation. For the stability of the system under the perturbation the absence of such poles is therefore crucial.

JHEP09(2007)057

The time and space dependence of the field is given by simple exponentials

$$\phi(t,x) \sim \mathrm{e}^{-i\omega t}\,\mathrm{e}^{iqx}\,,$$

where $q := q^R + iq^I$. We will distinguish between the cases $x > 0$ and $x < 0$.

For $x > 0$ stability demands an exponentially decaying wave and therefore $\operatorname{sign} q^I = +1$. We further demand that the wave is outgoing from the origin of the perturbation which demands $\operatorname{sign}\omega = \operatorname{sign} q^R$. Taking these two facts together amounts to the condition

$$\operatorname{sign}\left(\frac{\omega}{q^R}\right) = \operatorname{sign} q^I\ . \tag{2.8}$$

Doing the same analysis for $x < 0$, one finds that the perturbation moves away to the left if $\operatorname{sign}\omega = -\operatorname{sign} q^R$, whereas the stability condition is now $\operatorname{sign} q^I = -1$. This again amounts to eq. (2.8).

We want to prove now that in the gravity dual the complex momentum modes of the black hole follow indeed the rule given by equation (2.8). We consider a minimally coupled scalar Φ in $\mathrm{AdS}_5 \times \mathrm{S}^5$ with mass m. The line element of the AdS black hole with planar horizon is

$$\mathrm{d}s^2_{\mathrm{AdS}} = \frac{r^2}{R^2}\left(-f(r)\mathrm{d}t^2 + \mathrm{d}\mathbf{x}^2\right) + \frac{R^2}{r^2 f(r)}\,\mathrm{d}r^2\,, \tag{2.9}$$

where $f(r) = 1 - (r_{\mathrm{H}}/r)^4$. The temperature is given through $r_{\mathrm{H}} = \pi R^2 T$. We will use in the following the coordinate $z = r_{\mathrm{H}}/r$ and rescale time and space coordinates by $r_{\mathrm{H}} R^{-2}(t,\mathbf{x}) \mapsto (t,\mathbf{x})$. The boundary is now located at $z = 0$ and the horizon at $z = 1$. The equation of motion for a minimally coupled scalar $\Phi(t,z,x) = \exp(-i\omega t + iqx)\,\Phi(z)$ of mass m is

$$\Phi'' + \left(\frac{f'(z)}{f(z)} - \frac{3}{z}\right)\Phi' + \left(\frac{\omega^2}{f(z)^2} - \frac{q^2}{f(z)} - \frac{m^2}{z^2 f(z)}\right)\Phi(z) = 0\ . \tag{2.10}$$

We can further split $\Phi(z) = \sigma(z)\,y(z)$, in order to find an equation for $y(z)$ that is Schrödinger-like in a 'tortoise' z_* coordinate defined through

$$\mathrm{d}z_* = \frac{\mathrm{d}z}{f(z)} \quad \Rightarrow \quad \Big(\partial^2_{z_*} + \omega^2 - V(z_*)\Big)y(z_*) = 0\,, \tag{2.11}$$

provided that $\sigma(z)$ fulfils

$$\frac{\sigma'(z)}{\sigma(z)} = \frac{3}{2z}\ . \tag{2.12}$$

In the z coordinate the Schrödinger potential reads

$$V(z) = \frac{f(z)}{4z^2}\Big(15 + 4m^2 + 4q^2 z^2 + 9z^4\Big) := V_0(z) + \mathrm{Re}(q^2)\,f(z) + i\,\mathrm{Im}(q^2) f(z)\,, \tag{2.13}$$

where we have separated it into its real and imaginary parts. In the z_* coordinate the horizon lies at $z_* \to +\infty$ and the potential vanishes there, so the wavefunction can be described as a superposition of plane waves. The infalling boundary condition corresponds to setting $y(z_*) = \mathrm{e}^{i\omega z_*}\,\chi(z_*)$ with $\chi(+\infty) = \text{const}$. Thus we find

$$\Big(\partial^2_{z_*} + 2i\omega\,\partial_{z_*} - V_0(z_*) - \mathrm{Re}(q^2)\,f(z_*) - i\,\mathrm{Im}(q^2)\,f(z_*)\Big)\,\chi(z_*) = 0\ . \tag{2.14}$$

If we multiply by the conjugate $\overline{\chi}(z_*)$ and pick out the imaginary part of the equation we obtain

$$-\frac{i}{2}\left(\overline{\chi}\partial_{z_*}^2\chi - \chi\partial_{z_*}^2\overline{\chi}\right) + \omega\,\partial_{z_*}|\chi|^2 - \mathrm{Im}(q^2)f(z_*)|\chi|^2 = 0\,, \tag{2.15}$$

Now we integrate this equation between the boundary ($z_* = z_*^b$) and the horizon ($z_* = +\infty$). Upon a partial integration the derivative terms cancel each other: $\chi(z_*)$ vanishes at the boundary due to the Dirichlet boundary condition we impose there and at the horizon the derivative vanishes $\partial_{z_*}\chi(+\infty) = 0$. The remaining terms in equation (2.15) amount to

$$\omega\,|\chi(z=1)|^2 = \mathrm{Im}(q^2)\int_{z_*^b}^{\infty}\mathrm{d}z_*\,f(z_*)|\chi(z_*)|^2 = \mathrm{Im}(q^2)\int_0^1\mathrm{d}z\,|\chi(z)|^2\,, \tag{2.16}$$

The integral on the right hand side is positive definite, which then implies that $\mathrm{sign}\,\omega = \mathrm{sign}\,\mathrm{Im}(q^2) = \mathrm{sign}(q^R q^I)$ which is precisely the stability condition (2.8).

There is a further stability condition involving the properties of the potential. When $\omega = 0$, we have the condition that $\mathrm{Im}(q^2) = 0$, so either $q^R = 0$ or $q^I = 0$. Consider now the real part of the Schrödinger equation (2.14). After multiplying by $\overline{\chi}(z_*)$ and integrating between the boundary and the horizon we find

$$\int_{z_*^b}^{\infty}\mathrm{d}z_*\left(|\partial_{z_*}\chi(z_*) + i\omega\chi(z_*)|^2 + (V_0(z_*) - \omega^2)|\chi(z_*)|^2\right) = -\,\mathrm{Re}(q^2)\int_0^1\mathrm{d}z\,|\chi(z)|^2\,, \tag{2.17}$$

Clearly, if $V_0(z_*) \geq 0$ between the boundary and the horizon, then, at $\omega = 0$, $\mathrm{Re}(q^2) < 0$ and we will have $q^R = 0$ and $q^I \neq 0$. On the other hand, if the potential is negative on some region, then there could be solutions with $\mathrm{Re}(q^2) > 0$ or equivalently $q^R \neq 0$ and $q^I = 0$. Considering four-dimensional Minkowski slices of AdS_5, these modes can be regarded as tachyonic instabilities of negative mass squared $m^2 = -(q^R)^2$. Notice that with our choice the boundary conditions $\sim \mathrm{e}^{i\omega z_*}$ and fixing ω to be real, this condition actually refers to the presence of 'negative energy' modes in the scattering spectrum, so only when the potential is negative at the horizon this kind of instabilities could appear. Other instabilities associated to the presence of bound states could be present, see the appendix A for a discussion.

If $\mathrm{Re}(q^2) > 0$ instabilities are present in the bulk theory, the gauge correlation functions associated to the dual operators will show an oscillatory behavior at large separations, as opposed to vanishing, indicating that the plasma is actually out of equilibrium. From the point of view of the effective three-dimensional theory, instabilities will appear as tachyonic states in the spectrum.

3. Absorption lengths: numerical analysis

3.1 Scalar operators

As a first example we want to compute the absorption lengths of a scalar operator $\mathcal{O}(t, \mathbf{x})$ of conformal dimension $\Delta = 4$. We choose this particular case because it is the simplest setup we can use to illustrate the method, since the dual supergravity field corresponds to

JHEP09(2007)057

a minimally coupled, massless scalar. A possible example is given by $\mathcal{O} = \mathrm{tr}F^2$, that maps to the dilaton in the holographic dual.

Consider the retarded two-point correlation function in the theory attemperature T

$$G_{\mathrm{R}}(t-t', \mathbf{x}-\mathbf{y}) = -i\,\theta(t-t')\,\left\langle [\mathcal{O}(t,\mathbf{x}), \mathcal{O}(t',\mathbf{y})] \right\rangle \ . \tag{3.1}$$

At large distances $|\mathbf{x}-\mathbf{y}| \gg T^{-1}$, the Green's function decays exponentially due to thermal screening. As we have explained, this behavior is determined by a set of discrete lengths that in linear response theory describe the *absorption* of out-of-equilibrium perturbations. For the theory in equilibrium they are identified with *correlation lengths* in the plasma, as proposed in ref. [20]. The squared inverse of the zero-frequency correlation lengths can also be regarded as the glueball masses[6] of a three-dimensional effective theory in the high-temperature limit [17 – 19]. Via AdS/CFT correspondence we can reduce this complicated non-perturbative problem in the gauge theory to finding the complex momenta that allow the dilaton fluctuations to obey infalling boundary conditions on the horizon and Dirichlet ones on the boundary. In this example, and in the other cases we consider in this paper, the equations of motion can be reduced to Heun equations that we can solve using semi-analytic methods.

The equation of motion for this field was already derived in subsection 2.1. Throughout the paper we use dimensionless frequency and momentum. In order to recover the dimensionful quantities it is enough to make the substitution $(\omega, \mathbf{q}) \mapsto \pi T\,(\omega, \mathbf{q})$. Changing coordinates from z to $x = 1 - z^2$, the equation now reads

$$\Phi'' + \frac{1+(1-x)^2}{x(1-x)(2-x)}\,\Phi' + \left(\frac{\omega^2}{4x^2(1-x)(2-x)^2} - \frac{q^2}{4x(1-x)(2-x)}\right)\Phi(x) = 0\ . \tag{3.2}$$

This equation has four regular singular points at $x = 0, 1, 2, \infty$, with characteristic exponents

$$\{0; -i\omega/4, +i\omega/4\}\,, \quad \{1; 0, 2\}\,, \quad \{2; -\omega/4, +\omega/4\}\,, \quad \{\infty; 0, 0\}\ .$$

Therefore, we can transform it into a Heun equation and we can follow the analysis described in [12]. To compute the complex wave numbers we simply have to analytically continue the momentum instead of the frequency. It is interesting to observe that none of the characteristic exponents at the singular points depend on the momenta. We factorize $\Phi(x)$ as

$$\Phi(x) = x^{-i\omega/4}\,(1-x)^2\,(2-x)^{-\omega/4}\,y(x)\,, \tag{3.3}$$

which allows us to write the equation of motion in the standard form of a Heun equation for $y(z)$

$$y''(x) + \left(\frac{\gamma}{x} + \frac{\delta}{x-1} + \frac{\epsilon}{x-2}\right)y'(x) + \frac{\alpha\beta x - Q}{x(x-1)(x-2)}\,y(x) = 0\,, \tag{3.4}$$

with parameters

$$\alpha = \beta = 2 - \frac{\omega}{4}(1+i)\,, \quad Q = 4 + \frac{q^2}{4} - (1+7i)\frac{\omega}{4} - (2-i)\frac{\omega^2}{8}\,, \tag{3.5}$$

$$\gamma = 1 - i\frac{\omega}{2}\,, \quad \delta = 3\,, \qquad \epsilon = 1 - \frac{\omega}{2}\ . \tag{3.6}$$

[6] In this particular example we are considering $J^{\mathrm{PC}} = 0^{++}$ glueballs.

All the other perturbations we will consider in this paper can be transformed to Heun equations in a similar way. In [13] the same perturbations have been studied in order to solve for the quasinormal modes. The solution $y_0(x)$ corresponding to the infalling boundary conditions at the horizon $x = 0$ is a linear combination of local solutions $y_{1,A}$,$y_{1,B}$ at $x = 1$

$$y_0(x) = A\, y_{1,A}(x) + B\, y_{1,B}(x)\,, \tag{3.7}$$

where $y_{1,A}$ is analytic at $x = 1$. The retarded Green's function turns out to be proportional to

$$G_{\rm R} \propto \frac{A}{B}\,, \tag{3.8}$$

and the poles correspond therefore to the solutions with $B = 0$, i.e. solutions that are analytic in the interval $x \in [0, 1]$. These boundary conditions determine a discrete set of complex momentum eigenvalues if we fix the frequency ω to real values.

We can find local solutions using the Frobenius method close to the singularities. In the cases under consideration, a solution with boundary condition $y(0) =$ const. will be a superposition of solutions with exponents $1 - \delta \leq 0$ and 0 close to the AdS boundary ($x = 1$). The boundary condition $y(1) =$ const. can be satisfied only for a discrete set of frequencies ω or momenta q. These values can be computed imposing matching conditions at some intermediate point for the Frobenius series although we will need a large number of terms and the convergence gets worse for higher frequencies. There is an alternative method based on the improved convergence of the solutions. Normal solutions are convergent for $|x| < 1$, but for some values of the parameters the solutions can converge for $|x| < 2$. This condition of extended convergence boils down to a transcendental equation for the frequencies or momenta in the form of a continued fraction (see [27, 12] for more details) using Pincherle's theorem on the existence of minimal solutions to three term recursion relations.

The coefficients of the Frobenius series at $x = 0$ should satisfy the recursion relation

$$a_{n+2} + A_n(\omega, q)\, a_{n+1} + B_n(\omega, q)\, a_n = 0\,, \quad n \geq 0\,, \tag{3.9}$$

where

$$A_n(\omega, q) = -\frac{(n+1)(2\delta + \epsilon + 3(n+\gamma)) + Q}{2(n+2)(n+1+\gamma)}\,, \tag{3.10}$$

$$B_n(\omega, q) = \frac{(n+\alpha)(n+\beta)}{2(n+2)(n+1+\gamma)}\,, \tag{3.11}$$

and $a_0 = 1,\ a_1 = Q/2\gamma$. Then, using the recursive definition

$$r_n = \frac{a_{n+1}}{a_n} = -\frac{B_n(\omega, q)}{A_n(\omega, q) + r_{n+1}}\ . \tag{3.12}$$

Pincherle's theorem states that a minimal solution to the three term recursion relation (3.10) exists if and only if the continued fraction on the right hand side in (3.12) converges. Moreover, in this case it converges precisely to a_{n+1}/a_n. In [12, 13] it was pointed out that the minimal solution corresponds precisely to a solution of the Heun

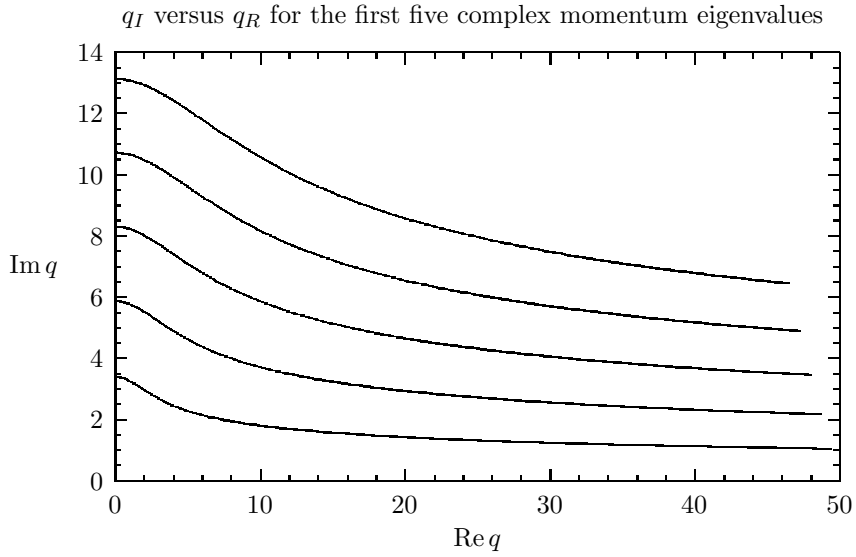

Figure 3: We have traced the locations of the five lowest momentum eigenvalues in the complex q-plane for different frequencies as a function of the frequency out to $\omega = 50$. The momentum eigenvalues vary continuously with the frequency and lie on the analogues of Regge trajectories.

equation that is analytic at $x = 1$ therefore fulfilling the correct boundary conditions. Choosing $n = 0$ we find

$$r_0 = \frac{Q}{2\gamma} \,, \tag{3.13}$$

and computing r_0 recursively gives a transcendental equation for q. Using this formula, we can compute numerically the complex momentum modes with high precision. In order to do that, we cut the fraction at a large value $n = n_* = 100$ and use the asymptotic value $r_n = 1/2 - (2 + \omega)/4n_*$. It is important to realize that Pincherle's theorem applies only if we are dealing with genuine three term recursion relations. Sometimes it can happen that the recursion relation involves three terms only from a certain value of $n = n_1$ on. This happens for example if either $\alpha = 0$ or $\beta = 0$ when $B_0 = 0$. In such a case one has to use (3.12) with $n = n_1$. We will see that we are faced with this in the cases of the longitudinal vector field perturbations and of the shear mode perturbations at $\omega = 0$. Since $\alpha = 0$ in both cases it is sufficient to take $n_1 = 1$ and use

$$r_1 = \frac{Q^2 + 3Q\gamma - 2\alpha\beta\gamma + 2Q\delta + Q\epsilon}{4Q + 4Q\gamma} \,, \tag{3.14}$$

instead of (3.13).

We have numerically computed the complex momentum eigenvalues using this method. The results for the scalar field perturbations are shown in figure 4. The real and imaginary parts of the five lowest complex momentum are plotted as a function of the frequency. The real parts start out at $q^R = 0$ for zero frequency. The imaginary parts start out at a finite value at $\omega = 0$, develop a shoulder that is more pronounced for the higher

n	q_n^2
1	-11.5877
2	-34.5270
3	-68.9750
4	-114.9104
5	-172.3312
6	-241.2366
7	-321.6265
8	-413.5009
9	-516.8597
10	-631.7028

Table 1: The first ten glueballs of the scalar mode.

modes and then fall off rather fast until they enter a regime of slow decrease for large frequencies. Numerically we found that the lowest mode becomes almost constant at large frequencies with $q^I \approx 0.83$ at $\omega = 100$. Also the higher modes flatten out for high frequencies. As expected, higher frequencies can penetrate farther into the plasma. It is an interesting question if the plasma becomes transparent for some high but finite frequency, if transparency is reached only in the limit $\omega = \infty$ or if the absorption length stays finite. Unfortunately our algorithm does not allow us to explore this asymptotic regime. We can speculate however using the underlying conformal invariance of the $\mathcal{N}=4$ theory. Since for high frequencies the temperature is less and less important we expect that the absorption length diverges as $\omega \to \infty$, i.e. $q^I(\omega = \infty) = 0$. A finite absorption length would point to an underlying scale in the theory. On the other hand, if the plasma were to become transparent at some finite value of ω, we would expect that to happen at a scale that is set by the temperature. However, our numerical results show finite absorption lengths for much higher frequencies.

3.1.1 Glueball masses

Of particular interest are the absorption lengths in the static limit $\omega \to 0$. In this case we will refer to the absorption length as the screening length. The equation (3.2) with $\omega = 0$ has been studied before in [17, 18]. There the interpretation of the eigenvalues in the momentum with $q^2 < 0$ was as masses of glueballs in the three dimensional theory that is obtained by reduction on the thermal circle in the Euclidean section of the AdS black hole. The glueball masses can be calculated as the discrete eigenvalues $M_n^2 = -q_n^2$. Our numerical results at $\omega = 0$ for the first ten modes are compiled in table 1 and are in good agreement with results given by refs. [17, 18].

It is important to see if the eigenfunctions correspond to the wave functions of the glueballs too. In [19] the authors observe that for all the glueball masses the correct boundary conditions correspond to demanding analyticity of the wave function at the horizon and the boundary. These are precisely the same boundary conditions that emerge

in our case at $\omega = 0$. Therefore the screening lengths for static fields corresponds precisely to the glueball masses computed earlier in [17 – 19].

3.2 Global currents

In the $\mathcal{N}=4$ theory, the global currents associated to R-charges map to mixed components of the S^5 and AdS_5 metrics, that can be seen as graviphotons after dimensional reduction to AdS_5. In general, any global symmetry in the field theory will map to a local gauge symmetry in the holographic dual. Then, to find the poles of the retarded Green functions in the plasma

$$G_{\mu\nu}(t-t', \mathbf{x}-\mathbf{y}) = -i\,\theta(t-t')\,\left\langle [J_\mu(t,\mathbf{x}), J_\nu(t',\mathbf{y})] \right\rangle\,, \tag{3.15}$$

we have to compute the complex momentum eigenvalues for vector fields in the AdS black hole.[7] We will see that there are two decoupled sectors, corresponding to transverse and longitudinal channels. The reason is that temperature breaks four-dimensional Lorentz symmetry to three-dimensional rotational symmetry. In the glueball language, the zero-frequency masses correspond to $J^{\rm PC} = 1^{--}$ and 0^{-+} states. However the states arising from the vector fields are also charged under the global R-symmetry and therefore do not form part of the superselection sector that constitutes QCD_3. For simplicity we will refer to these states also as glueballs. The longitudinal channel is special because it also describes the diffusion of the conserved charge through the plasma, that does not appear as a glueball state in the three-dimensional theory because the residue of the diffusion mode vanishes in the zero-frequency limit. We will show that the diffusion pole is also captured by complex momentum eigenvalues.

We can compute the complex momentum eigenvalues corresponding to a vector field in the AdS-Schwarzschild background in an analogous way to the scalar field case. The equations of motion for such a field are given by the Maxwell equations

$$\frac{1}{\sqrt{-g}}\partial_\nu\left[\sqrt{-g}\,g^{\mu\rho}g^{\nu\sigma}F_{\rho\sigma}\right] = 0\,, \tag{3.16}$$

where $F_{\mu\nu} = \partial_\mu A_\nu - \partial_\nu A_\mu$. We can choose the $A_z = 0$ gauge in the metric (2.9) and expand in plane waves A_μ. Separating the vector field in longitudinal and transverse components, $A_L(z) = \frac{\mathbf{q}}{q}\cdot\mathbf{A}(z)$ and $\mathbf{q}\cdot\mathbf{A}_T(z) = 0$, the equations of motion are

$$0 = \omega A_0'(z) + f(z) q A_L'(z)\,, \tag{3.17}$$

$$0 = A_0''(z) - \frac{1}{z}A_0'(z) - \frac{1}{f(z)}\Big(\omega q A_L(z) + q^2 A_0(z)\Big)\,, \tag{3.18}$$

$$0 = A_L''(z) + \frac{z}{f(z)}\left(\frac{f(z)}{z}\right)' A_L'(z) + \frac{1}{f(z)^2}\Big(\omega q A_0(z) + \omega^2 A_L(z)\Big)\,, \tag{3.19}$$

$$0 = \mathbf{A}_T''(z) + \frac{z}{f(z)}\left(\frac{f(z)}{z}\right)' \mathbf{A}_T'(z) + \left(\frac{\omega^2}{f(z)^2} - \frac{q^2}{f(z)}\right)\mathbf{A}_T(z)\,. \tag{3.20}$$

The first three equations are not independent so we can use the first one to write decoupled equations for $A_0'(z)$ and $A_L'(z)$. Notice that there is a choice of gauge invariant variables

[7] We are assuming that the total charge in the equilibrium state vanishes, so there are no chemical potentials.

JHEP09(2007)057

$E_L = qA_0 + \omega A_L$ and $\mathbf{E}_T = \omega \mathbf{A}_T$ that describe the diffusive and transverse channel respectively [8]. However, the spectrum of complex momentum values (equivalently of quasinormal modes) is gauge invariant, so it should not matter if we choose to work with gauge components, that obey simpler equations. Since the invariant quantity is E_L, this means that A_0 and A_L should have the same spectrum, as the constraint (3.17) points out.

Then, the relevant equations for the temporal, longitudinal and transverse components of the vector field read

$$0 = V_0'' + \left(\frac{f'}{f} - \frac{1}{z}\right) V_0' + \left(\frac{\omega^2}{f^2} - \frac{q^2}{f} - \frac{f'}{zf} + \frac{1}{z^2}\right) V_0(z)\,, \tag{3.21}$$

$$0 = V_L'' + \left(3\frac{f'}{f} - \frac{1}{z}\right) V_L' + \left(\frac{\omega^2}{f^2} - \frac{q^2}{f} + \left(\frac{f'}{f}\right)^2 + \frac{f''}{f} - 2\frac{f'}{zf} + \frac{1}{z^2}\right) V_L(z)\,, \tag{3.22}$$

$$0 = \mathbf{A}_T'' + \left(\frac{f'}{f} - \frac{1}{z}\right) \mathbf{A}_T' + \left(\frac{\omega^2}{f^2} - \frac{q^2}{f}\right) \mathbf{A}_T(z)\ , \tag{3.23}$$

where we define $V_0(z) = A_0'(z)$, $V_L(z) = A_L'(z)$. In the $x = 1 - z^2$ coordinate and for a suitable factorization of each component, the equations above can be written as Heun equations:

Temporal. The critical exponents at the singularities are

$$\left(0; -i\frac{\omega}{4}, i\frac{\omega}{4}\right)\,, \quad \left(1; \frac{1}{2}, \frac{1}{2}\right)\,, \quad \left(2; -\frac{\omega}{4}, \frac{\omega}{4}\right)\,, \quad \left(\infty; -\frac{1}{2}, \frac{3}{2}\right)\ .$$

$$V_0(x) = x^{-i\omega/4}(x-1)^{1/2}(x-2)^{-\omega/4} y(x)\ . \tag{3.24}$$

Longitudinal. The critical exponents at the singularities are

$$\left(0; -1 - i\frac{\omega}{4}, -1 + i\frac{\omega}{4}\right)\,, \quad \left(1; \frac{1}{2}, \frac{1}{2}\right)\,, \quad \left(2; -1 - \frac{\omega}{4}, -1 + \frac{\omega}{4}\right)\,, \quad \left(\infty; \frac{5}{2} - \sqrt{5}, \frac{5}{2} + \sqrt{5}\right)\ .$$

$$V_L(x) = x^{-1-i\omega/4}(x-1)^{1/2}(x-2)^{-1-\omega/4} y(x)\ . \tag{3.25}$$

In both cases we find the same parameters for the Heun equation

$$\begin{aligned} &\alpha = -\frac{\omega}{4}(1+i)\,, \quad \beta = 2 - \left(\frac{\omega}{4}(1+i)\right)\,, \quad Q = \frac{q^2}{4} - (1+3i)\frac{\omega}{4} - (2-i)\frac{\omega^2}{8}\,, \\ &\gamma = 1 - i\frac{\omega}{2}\,, \qquad \delta = 1\,, \qquad \epsilon = 1 - \frac{\omega}{2}\ . \end{aligned} \tag{3.26}$$

Notice that the boundary conditions for $V_L(x)$ are not infalling ones. They are determined by the constraint 3.17.

Transverse. The critical exponents at the singularities are

$$\left(0; -i\frac{\omega}{4}, i\frac{\omega}{4}\right)\,, (1; 0, 1)\,, \quad \left(2; -\frac{\omega}{4}, \frac{\omega}{4}\right)\,, \quad (\infty; 0, 1)$$

$$A_T(x) = x^{-i\omega/4}(x-1)(x-2)^{-\omega/4} y(x)\ .$$

$$\begin{aligned} &\alpha = 1 - \frac{\omega}{4}(1+i)\,, \quad \beta = 2 - \left(\frac{\omega}{4}(1+i)\right)\,, \quad Q = \frac{q^2}{4} + 2 - (1+5i)\frac{\omega}{4} - (2-i)\frac{\omega^2}{8}\,, \\ &\gamma = 1 - i\frac{\omega}{2}\,, \qquad \delta = 2\,, \qquad \epsilon = 1 - \frac{\omega}{2}\ . \end{aligned} \tag{3.27}$$

JHEP09(2007)057

n	q_n^2
1	-5.1313
2	-22.4816
3	-51.2098
4	-91.4106
5	-143.0926
6	-206.2577
7	-280.9066
8	-367.0395
9	-464.6566
10	-573.7580

Table 2: The first ten glueballs of the transverse mode.

As we had anticipated, the temporal and longitudinal components have the same spectrum, since they obey the same Heun equation, although this was not evident in equations (3.21) and (3.22). The results are shown in figures 5 and 6. The real and imaginary parts of the five lowest complex momentum are plotted as a function of the frequency. The behavior is similar to the one found for the scalar operator. The imaginary parts start out at a finite value at $\omega = 0$, develop a shoulder that is more pronounced for the higher modes and then fall off rather fast until they enter a regime of slow decrease for large frequencies. The real parts start out the $q^R = 0$ for zero frequency.

So far, we have described the absorption of R-current excitations in the plasma. However, a conserved global charge cannot be dissipated, it is spread out by the slow process of diffusion. This is described in the hydrodynamic regime $\omega, q \ll T$ by a diffusion pole [25] (units restored)

$$\omega = -i\,\frac{q^2}{2\pi T}\ . \tag{3.28}$$

In our analysis of complex wave numbers we are able to see numerically this mode ($q = (1+i)\sqrt{\omega}$ with our conventions) that fits nicely with the analytic prediction in the hydrodynamical regime figure 8.

3.2.1 Glueball masses

In the zero frequency limit, the absorption lengths can be interpreted as the inverse glueball masses of an effective three-dimensional theory. Note however that these states do not lie in the superselection sector that constitutes the holographic dual of QCD_3! For the longitudinal channel we have to take into account that $\alpha(\omega = 0) = 0$ so we have to use the modified recursion relation starting at $n = 1$ (3.14). It turns out that the glueball masses of the longitudinal channel coincide with the ones found for the scalar operator, table 1. Indeed, at $\omega = 0$ we can transform the Heun equation with parameters (3.5) into the Heun equation with parameters (3.26). First, make the coordinate transformation $x \to \frac{x-2}{x-1}$, that shuffles the singular points $2 \leftrightarrow 0$, $1 \leftrightarrow \infty$. Then, the redefinition $y(x) \to (x-1)^2 y(x)$

(explained in the appendix) shows that both equations are equivalent. Notice that the solutions that are analytic in $[0,1]$ in the transformed equation correspond to solutions that are analytic in $[2,\infty]$ in the original equation, and not to the physical modes. However, such solutions can be generated from the physical ones by conformal transformations on the two sphere,[8] so both types appear for the same values of the parameters. Notice that the both solutions have a similar analytic structure, the only singularity is a branch cut joining two of the singular points. Also the fact that the auxiliary parameters Q of both equations are the same for the particular cases we are considering, allows an immediate identification of the complex momentum numbers.

The transverse channel has different spectrum, whose first modes are in table 2. Although the glueballs associated to vector fields have non-zero R-charge, and are usually not considered, our computation shows that the lightest three-dimensional state and hence, the longest correlation length, belongs to this class.[9]

3.3 Stress-energy tensor

The stress-energy tensor of the gauge theory encodes important dynamical and thermodynamical properties of the plasma. Correlation functions of the stress-energy tensor

$$G_{\mu\nu,\rho\sigma}(t-t',\mathbf{x}-\mathbf{y}) = -i\,\theta(t-t')\,\left\langle [T_{\mu\nu}(t,\mathbf{x}),T_{\rho\sigma}(t',\mathbf{y})]\right\rangle\,, \tag{3.29}$$

are related to perturbations of the metric that leave the S^5 factor invariant. Therefore, we want to introduce a small fluctuation of the four-dimensional part of the metric $g_{\mu\nu} = g^0_{\mu\nu} + h_{\mu\nu}$.

In the gauge theory, the breaking of Lorentz symmetry to rotational symmetry by temperature splits the Green's functions in transverse, shear and sound channels, that in the zero frequency limit contain the $J^{\rm PC} = 2^{++}$, 1^{++} and 0^{++} glueball spectrum. This is reflected in the gravity dual, where the perturbations fall into three different classes with decoupled field equations [25, 26, 8]. The associated spin to each of these channels is also 2, 1 and 0, so we will refer to them also as tensor, vector and scalar.

In the shear and sound channels there are also hydrodynamical modes that describe the diffusion of conserved momentum and the propagation of sound. We will not study the sound channel, but we will show that complex momentum modes also capture the shear pole. We will work with gauge-invariant variables, following [23]. There, the authors consider general metrics of the form

$$\mathrm{d}s^2 = -\mathsf{F}(r)\,\mathrm{d}t^2 + \frac{\mathrm{d}r^2}{\mathsf{F}(r)} + r^2\mathrm{d}\sigma_n^2\,, \tag{3.30}$$

where $\mathrm{d}\sigma_n^2$ corresponds to a metric of a n-dimensional space of constant sectional curvature $K = 0, \pm 1$, and

$$\mathsf{F}(r) = K - \frac{2M}{r^{n-1}} - \lambda r^2\ . \tag{3.31}$$

[8] See [30] for an exhaustive list of Heun solutions and their relations.

[9] This state is even lighter than the lightest QCD_3 glueball listed in [19].

JHEP09(2007)057

In our case, $K = 0$, $n = 3$, $\lambda = -1$ and $M = r_{\rm H}^4/2$.

The Einstein equations are decomposed in tensor, vector and scalar components relative to the three-dimensional metric. It is thus possible to define three different gauge-invariant quantities to which we can associate a Schrödinger-like equation of motion [23]. In the z coordinate it reads

$$-f(z)\,\frac{\mathrm{d}}{\mathrm{d}z}\left(f(z)\,\frac{\mathrm{d}\psi_I}{\mathrm{d}z}\right)+V_I(z)\,\psi_I=\omega^2\,\psi_I\,,\quad I\equiv\{T,V,S\}\,, \tag{3.32}$$

where for each perturbation we will have a different potential. Rewriting the Schrödinger equation by shifting $(\omega, q) \mapsto r_{\rm H}(\omega, q)$, the potentials V are given by

$$\begin{aligned}
V_T(z) &= \frac{f(z)}{4z^2}\,(15+4\,q^2z^2+9z^4)\,,\\
V_V(z) &= \frac{f(z)}{4z^2}\,(3+4\,q^2z^2-27z^4)\,,\\
V_S(z) &= \frac{f(z)}{4z^2}\,\frac{1}{(1+6q^{-2}z^2)^2}\left(-1+4\,q^2z^2+9z^4+156z^6-108\frac{z^2}{q^2}+540\frac{z^4}{q^4}+324\frac{z^8}{q^4}\right)\,,
\end{aligned} \tag{3.33}$$

for tensor, vector and scalar perturbations, respectively.

By making the change of variable $x = 1 - z^2$, the equations for tensor and vector perturbations lead to a Heun equation. For scalar perturbations the situation is not so simple, and it requires a separate analysis that we leave for future work, so in the following we will be concerned only with tensor and vector perturbations.

Tensor perturbations. The characteristic exponents are

$$\left(0;-i\frac{\omega}{4},i\frac{\omega}{4}\right)\,,\quad \left(1;-\frac{3}{4},\frac{5}{4}\right)\,,\quad \left(2;-\frac{\omega}{4},\frac{\omega}{4}\right)\,,\quad \left(\infty;\frac{3}{4},\frac{3}{4}\right)\,.$$

$$\psi_T(x)=x^{-i\omega/4}(x-1)^{5/4}(x-2)^{-\omega/4}y(x)\,. \tag{3.34}$$

$$\begin{aligned}
\alpha\beta &= \left(\frac{\omega}{4}(1+i)-2\right)^2\,,\quad Q=\frac{q^2}{4}+4-(2-i)\left((-1+3i)\frac{\omega}{4}+\frac{\omega^2}{8}\right)\,,\\
\gamma &= 1-i\,\frac{\omega}{2}\,,\quad \delta=3\,,\quad \epsilon=1-\frac{\omega}{2}\,.
\end{aligned} \tag{3.35}$$

Vector perturbations. The characteristic exponents are

$$\left(0;-i\frac{\omega}{4},i\frac{\omega}{4}\right)\,,\quad \left(1;-\frac{1}{4},\frac{3}{4}\right)\,,\quad \left(2;-\frac{\omega}{4},\frac{\omega}{4}\right)\,,\quad \left(\infty;-\frac{3}{4},\frac{9}{4}\right)\,.$$

$$\psi_V(x)=x^{-i\omega/4}(x-1)^{3/4}(x-2)^{-\omega/4}y(x)\,. \tag{3.36}$$

$$\begin{aligned}
\alpha\beta &= \frac{\omega}{4}(1+i)\left(\frac{\omega}{4}(1+i)-3\right)\,,\quad Q=\frac{q^2}{4}-(1+5i)\frac{\omega}{4}-(2-i)\frac{\omega^2}{8}\,,\\
\gamma &= 1-i\,\frac{\omega}{2}\,,\quad \delta=2\,,\quad \epsilon=1-\frac{\omega}{2}\,.
\end{aligned} \tag{3.37}$$

n	q_n^2
1	-18.6758
2	-47.4951
3	-87.7228
4	-139.4167
5	-202.5882
6	-277.2408
7	-363.3762
8	-460.9949
9	-570.0974
10	-690.6838

Table 3: The first ten glueballs of the shear mode.

Notice that tensor fluctuations obey the same equations as a massless scalar field, so the first modes of the spectrum are plotted in figure 4. The Heun equation we have for the vector perturbations goes over to the one the authors in [13] found for the shear mode after the transformation described in the appendix.

As we have commented above, vector fluctuations correspond to the shear channel of the gauge theory. This channel is associated to the momentum of the plasma, that as a conserved quantity is not absorbed but diffused. In the hydrodynamical limit it is possible to find an analytic expression for the diffusion pole [25]

$$\omega = -i\,\frac{q^2}{4\pi T}\ . \tag{3.38}$$

We find good numerical agreement for this mode $q = (1+i)\sqrt{2\omega}$, as can be seen in figure 9.

The results for the shear mode are shown in figure 7. The real and imaginary parts of the five lowest complex momentum are plotted as a function of the frequency. Again, we find a similar behavior to scalar and vector modes. The imaginary parts start out at a finite value at $\omega = 0$, develop a shoulder that is more pronounced for the higher modes and then fall off rather fast until they enter a regime of slow decrease for large frequencies. The real parts start out the $q^R = 0$ for zero frequency.

3.3.1 Glueball masses

We can find the glueball spectrum of the effective three-dimensional theory by taking the static limit $\omega = 0$. Again we have to use the recursion relation starting $n = 1$ (3.14) since $\alpha(\omega = 0) = 0$. The results for the shear channel are compiled in table 3. The glueball spectrum for neutral glueballs has been computed using a similar supergravity approach in [19]. The numbers we find differ actually somewhat from the ones quoted in [19] for the 1^{++} glueballs. We attribute this to the different numerical methods that have been used to obtain them.

JHEP09(2007)057

4. Conclusions and outlook

We have established a relation between solutions to linearized field equations with complex momenta in an AdS-black hole background and the absorption lengths of a conformal gauge theory in a plasma phase. We have explicitly studied some simple examples corresponding to scalar, vector and metric fluctuations. Due to conformal symmetry, all absorption lengths scale simply with T^{-1}. At zero frequency we find agreement with previous computations of the effective three-dimensional glueball spectrum [17 – 19]. However, we prefer in this paper to interpret our results as screening lengths for static fields. This interpretation has also recently and independently been proposed in ref. [20].

Furthermore, we have computed the dependence of the absorption length on the frequency. The results for the first modes are compiled in figures 4, 5, 6 and 7. In all the cases, the plasma is less absorptive for higher frequencies. The complex wave numbers also capture the hydrodynamical behavior for R-charge and momentum diffusion. Our numerical results are in agreement with the simple analytic continuation of the dispersion relation for the hydrodynamic modes. This is shown in figures 8 and 9.

One of the interesting results of our study is that the longest screening length (the lightest "glueball" mass in the dimensionally reduced theory) corresponds to a state with non-vanishing R-charge. Such a state does not belong to the spectrum of the QCD_3 theory, i.e. the mass gap of the effective three dimensional theory is not the one of QCD_3! Glueball masses play an important role in the determination of the Debye screening length. Here one studies the glueball exchange between open strings in the AdS black hole background. As has been pointed out in [20] the mass gap by itself is not important for the Debye screening, because only specific operators can couple to the open string. Since these open strings are R-charge neutral, the low mass states with non zero R-charge do not couple to the string. However, the string configuration one considers usually has its endpoints fixed on one point on the S^5 and it is also possible to consider strings that end on different points on the S^5. In such a situation the light non-zero R-charge states might become relevant and could modify the result for the screening length.

In this paper we have only studied the cases that can be reduced to Heun equations and allow the application of the efficient continued fraction approach to the calculation of the complex momentum eigenvalues. It would certainly be interesting to extend the present investigations to the cases that cannot be reduced to Heun equations. In these cases one has to resort to the elementary method of Frobenius expansions and this slows down the numerical calculation considerably. Nevertheless we think that this is an interesting problem especially in view of the comparison to the glueball mass calculations.

Another rather intersting point is the question whether the absorption length diverges in the limit of infinite frequency or whether it stays finite. Unfortunately so far we know only about numerical methods to evaluate the absorption lengths.

A related problem is the calculation of the absorption lengths in non-conformal holographic theories. Due to the presence of an underlying scale the dependence on the frequency is likely to show a more complicated pattern than the one we have found for the conformal case in this paper. It will also be of high interest to compute absorption lengths

JHEP09(2007)057

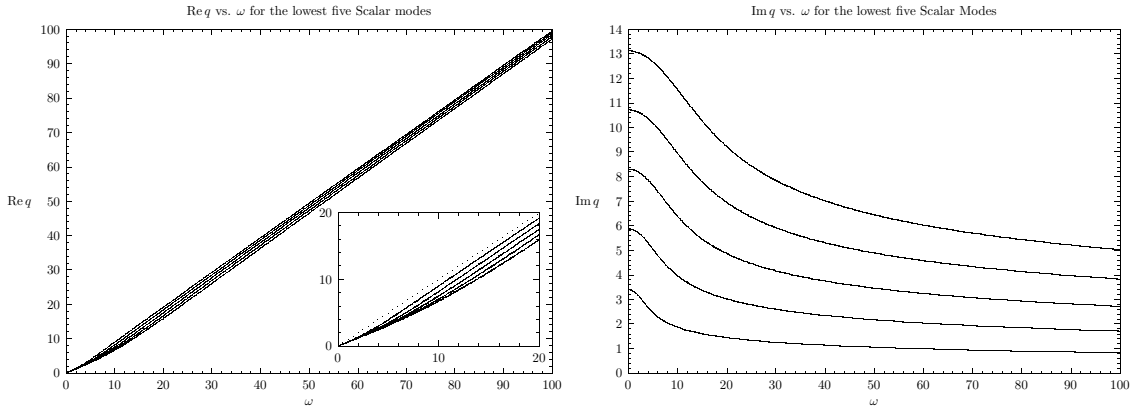

Figure 4: Real and imaginary parts of the lowest five complex momentum eigenvalues versus the frequency. In the lower-right corner of the first figure we have zoomed in to show the separation between the five modes.

for the meson states that appear in theories with D7-brane embeddings in the AdS black hole using the same methods that have been employed in the study of meson quasinormal modes in [28]. In [29] it has recently been emphasized that instabilities arise for near critical black hole embeddings. Such instabilities show up as quasinormal modes with positive imaginary part. As we have seen, similar instabilities can also arise in the study of the absorption lengths. Since the instabilities in the screening lengths arise at $\omega = 0$ and for real values of q^2 it might be much easier to search for these instead of unstable quasinormal modes!

We hope to make progress on these questions in future research.

Acknowledgments

The research of K. L. is supported by the Ministerio de Ciencia y Tecnología through a Ramón y Cajal contract. The research of S. M. is supported by an FPI 01/0728/2004 grant from Comunidad de Madrid. I. A. , K. L. and S. M. are supported in part by the Plan Nacional de Altas Energías FPA-2006-05485 and EC Commission under grant MRTN-CT-2004-005104. S. M. wants to thank the Physics Department at Swansea University for very warm hospitality. S. M. also wants to thank G. Sánchez for her support. We would like to thank G. Aarts, J. Barbón, P. Kumar, E. López, J. Mas and R. Schiappa for useful discussions.

A. Effective potentials

In section 2.1 we have presented the stability analysis for a scalar field but it can be generalized for any field component $\varphi(z)$ satisfying a decoupled linear second order differential equation

$$\varphi''(z) + A_1(z)\,\varphi'(z) + A_0(z)\,\varphi(z) + B(z)^2\omega^2\varphi(z) = 0\ . \tag{A.1}$$

JHEP09(2007)057

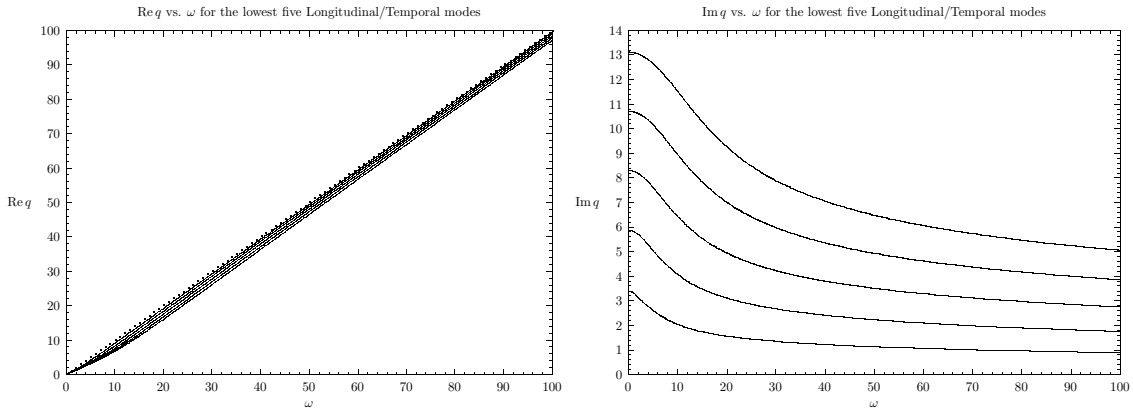

Figure 5: Longitudinal perturbations of the vector field on AdS. At $\omega = 0$ the values coincide with the ones of the scalar field perturbations. For $\omega > 0$ the shape is however different.

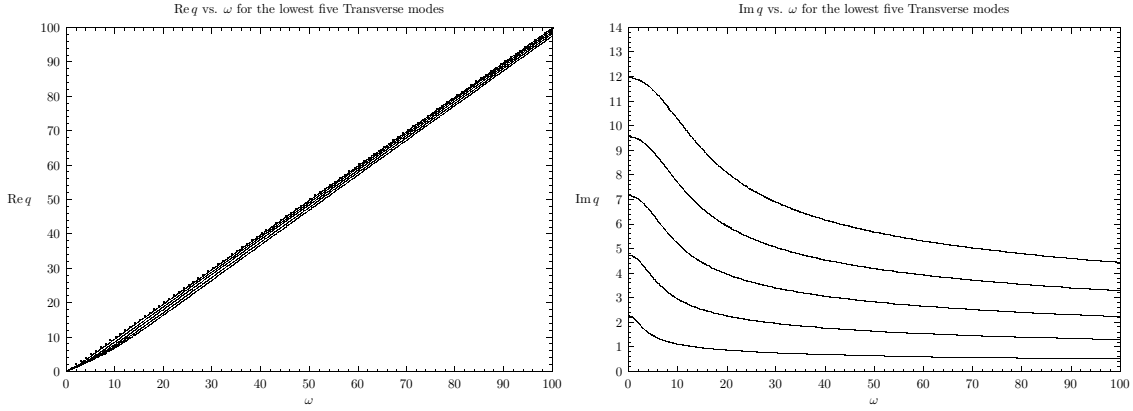

Figure 6: The complex momentum eigenvalues of the transverse vector field components. Note that the lowest mode gives the longest absorbtion length. The plasma is most transparent to transverse vector perturbations.

Factorizing $\varphi(z) = \sigma(z)\,\phi(z)$ and normalizing the ϕ'' term

$$\phi'' + \left(2\frac{\sigma'}{\sigma} + A_1\right)\phi' + \left(A_0 + A_1\,\frac{\sigma'}{\sigma} + \frac{\sigma''}{\sigma}\right)\phi + B(z)^2\omega^2\,f = 0\ . \tag{A.2}$$

We now change $B(z)\mathrm{d}z = \mathrm{d}z_*$ and divide by $B(z)^2$

$$\partial_{z_*}^2\phi + \omega^2\phi + \frac{1}{B(z)}\left(2\frac{\sigma'}{\sigma} + A_1 + \frac{B'(z)}{B(z)}\right)\partial_{z_*}\phi + \frac{1}{B(z)^2}\left(A_0 + A_1\,\frac{\sigma'}{\sigma} + \frac{\sigma''}{\sigma}\right)\phi = 0\ . \tag{A.3}$$

This expression becomes a Schrödinger equation when σ satisfies

$$2\frac{\sigma'}{\sigma} + A_1 + \frac{B'(z)}{B(z)} = 0\ . \tag{A.4}$$

JHEP09(2007)057

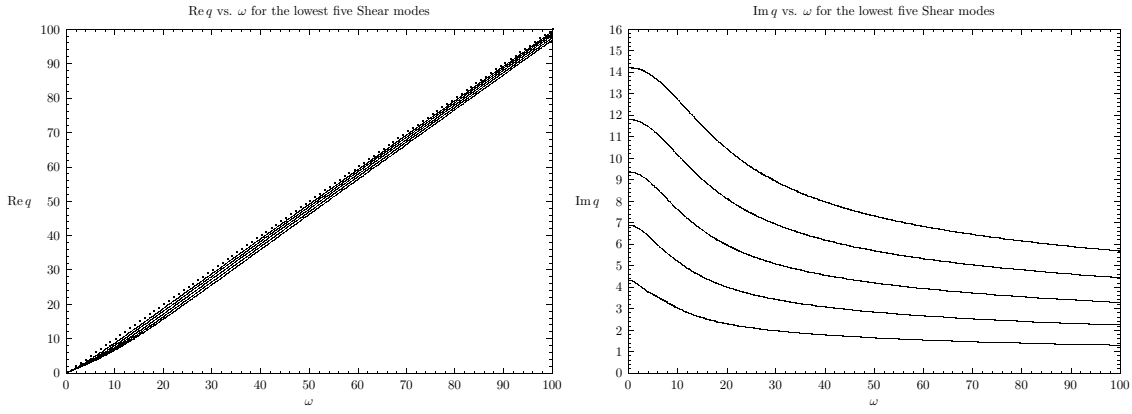

Figure 7: The lowest five complex momentum eigenvalues above the diffuse mode for the shear channel perturbations.

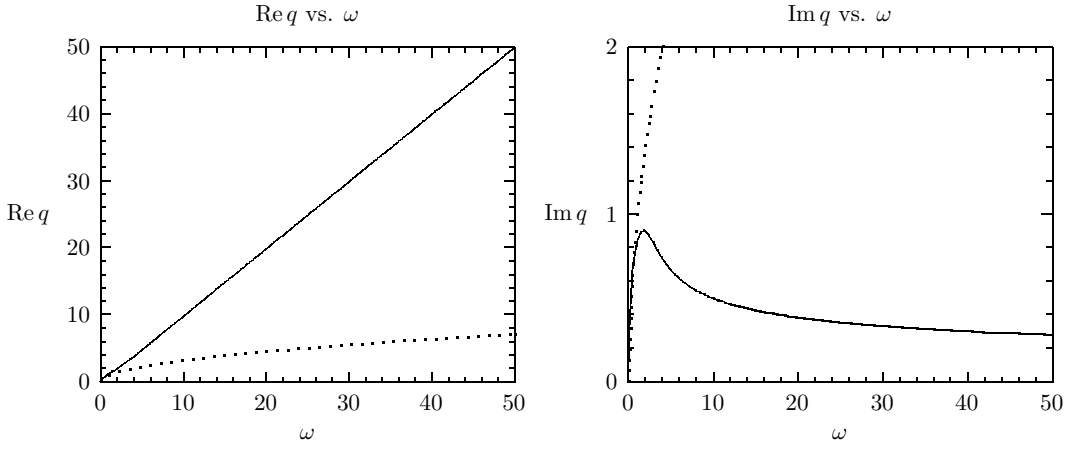

Figure 8: Diffusion mode. The solid line represents the numerical solution while the dotted line is the analytic formula from hydrodynamical analysis.

Then, the same stability arguments can be applied with the proper identification of the potential

$$V_0(z) = -\frac{1}{B(z)^2}\left(A_0 + \frac{1}{4}\left(\left(\frac{B'}{B}\right)^2 - A_1^2\right) - \frac{1}{2}\left(A_1' + \left(\frac{B'}{B}\right)'\right)\right) . \tag{A.5}$$

We will now apply this to the other equations under consideration in this paper.

- transverse vector components

$$V_0 = \frac{f(z)}{4z^2}\left(3 + 5z^4 + 4q^2z^2\right) , \tag{A.6}$$

- longitudinal and temporal vector components

$$V_0 = -\frac{f(z)}{4z^2}\left(1 + 7z^4 - 4q^2z^2\right) , \tag{A.7}$$

JHEP09(2007)057

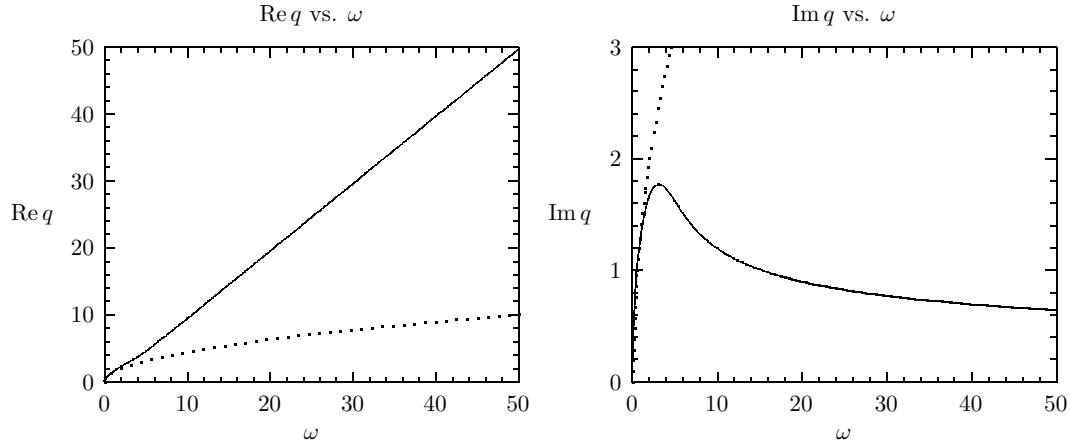

Figure 9: Shear mode. The solid line represents the numerical solution while the dotted line is the analytic formula from hydrodynamical analysis.

- gravitational vector perturbation (shear mode)

$$V_0 = \frac{f(z)}{4z^2}\left(3 - 27z^4 + 4q^2z^2\right) . \tag{A.8}$$

Due to the underlying analyticity of the solution of the corresponding Heun equation all fields, $\mathbf{A}_T, V_L, V_0, \Phi_V$, fulfill the boundary conditions leading to (2.16) and (2.17). The effective potential is positive in the case of the transverse vector fields. For the longitudinal and temporal vector field components it is negative and therefore the stability argument presented in section 2.1 does not apply. We note that the asymptotic behavior at the boundary is the same as that of a scalar field saturating the Breitenlohner-Freedman bound. We take this as an indication for stability, in the original analysis in AdS a positive energy condition is satisfied even for fields with negative potential [31]. The asymptotic behavior of the fields is restricted by the condition of having a well-defined conserved energy. In turn, the positive contribution of the kinetic energy always overcomes the negative contribution from the potential. A formal analysis [32] can be applied that shows the stability of vector perturbations. The 'Hamiltonian' operator $H = -\partial_{z_*}^2 + V_0$ must be positive definite over the set of normalizable solutions

$$\int_{z_*^b}^{\infty} \mathrm{d}z_* \chi^* H \chi > 0 . \tag{A.9}$$

We can rewrite (A.9) as

$$-\left[\chi^* D_\rho \chi\right]_{z_*^b}^{\infty} + \int_{z_*^b}^{\infty} \mathrm{d}z_* \left(|D_\rho \chi|^2 + V_\rho |\chi|^2\right) > 0 , \tag{A.10}$$

where we have introduced an auxiliary function ρ, such that $D_\rho = \partial_{z_*} + \rho$ and

$$V_\rho = V_0 + \partial_{z_*}\rho - \rho^2 . \tag{A.11}$$

A convenient election that makes $V_\rho \geq 0$ for vector fluctuations is $\rho = -f(z)/2z$. We can easily see that there is no contribution from the boundary term at the horizon, since $\chi(\infty) \to$ const. and $\rho(\infty) \to 0$. Therefore, we are left with the condition

$$\lim_{z\to 0} \chi^* \left(\partial_z - \frac{1}{2z}\right) \chi = 0 \ . \tag{A.12}$$

Close to the boundary, $V_0 \simeq -1/4z^2$, so the solution is a combination of Bessel functions $\chi \sim a\sqrt{z}J_0(\omega z) + b\sqrt{z}Y_0(\omega z)$. Then, the condition (A.12) satisfied when $b = 0$, that is equivalent to choose the normalizable solution at the boundary.

The effective potential of the shear mode is also interesting. It is negative close to the horizon. Equation (2.17) shows that this is a necessary requirement for existence of the hydrodynamic shear mode with $\mathrm{Re}(q^2) = 0$. We would expect that if the potential is deep enough, instabilities will appear. This is in agreement with other analysis that exhibit a negative well in the interior. Purely imaginary frequencies have been found in the study of electromagnetic and gravitational perturbations in global AdS [33, 34]. In the extremal limit, the frequencies seem to reach the real axis at $\omega = 0$, and the geometry was conjectured to be marginally unstable. Recent works also suggest that instabilities of D7 probe branes in AdS appear when a quasinormal mode crosses the real axis at $\omega = 0$ [28, 29].

B. Changing parameters in a Heun equation

In this appendix we show how to map a given Heun equation with given parameters into another Heun equation for a different function with a different set of parameters. This will allow in some cases to avoid the problem with "fake" modes.

Let us start with a Heun equation for $y(x)$

$$y'' + \left(\frac{\gamma}{x} + \frac{\delta}{x-1} + \frac{\epsilon}{x-2}\right) y' + \frac{\alpha\beta x - Q}{x(x-1)(x-2)}\ y(x) = 0\,, \tag{B.1}$$

where the parameters are subject to the condition $\alpha+\beta+1 = \gamma+\delta+\epsilon$. The characteristic exponents at the AdS boundary ($x = 1$) are in general

$$\{1; 0, 1-\delta\}\,,$$

for $y(x)$. In the cases where $\delta \in \{0 \cup \mathbb{Z}^-\}$, the first solution is logarithmic, but the logarithm might accidentally vanish at the "false frequencies"

$$y(x) = B[1 + (1-x) + \ldots + h(1-x)^{(1-\delta)}\log(1-x) + \ldots] + A[(1-x)^{(1-\delta)} + \ldots]\,, \tag{B.2}$$

where $h = 0$. According to [13], the Green's function is proportional to the ratio A/B, and the false frequencies are the ones for which accidentally $h = 0$.

Now we would like to change the function $y(x)$ such that we find a related Heun equation with different parameters. Let us define

$$y(x) = (1-x)^{\varrho}\, Y(x) \ . \tag{B.3}$$

This allows us to find a Heun equation for $Y(x)$, *provided* $\varrho = 1 - \delta$, and where the new set is

$$\begin{aligned}
\widetilde{\alpha} &= \alpha + \varrho = \alpha + 1 - \delta\,, \\
\widetilde{\beta} &= \beta + \varrho = \beta + 1 - \delta\,, \\
\widetilde{Q} &= Q + 2\gamma\varrho = Q + 2\gamma(1-\delta)\,, \\
\widetilde{\delta} &= \delta + 2\varrho = 2 - \delta\,, \\
\widetilde{\gamma} &= \gamma\,, \quad \widetilde{\epsilon} = \epsilon\,.
\end{aligned} \tag{B.4}$$

The interesting thing about this shift is that we can find a positive $\widetilde{\delta} \in \mathbb{Z}^+$ when in the original Heun equation we encounter fake frequencies. This always eliminates the false frequencies since the second solution is never analytic but goes like $(1-x)^{(\delta-1)}$, which is a negative (or zero) exponent for $\widetilde{\delta} \in \mathbb{Z}^+$. Now, the Frobenius solution is

$$Y(x) = B[(1-x)^{-\varrho} + \ldots + h(1-x)^{(1-\delta-\varrho)}\log(1-x) + \ldots] + A[(1-x)^{(1-\delta-\varrho)} + \ldots]\,. \tag{B.5}$$

The recursion algorithm of Leaver [27] and its adaption to the Heun equation by Starinets [12] computes when the solution of the Heun equation is analytic at $x = 1$. Now the solution that goes with the coefficient B is never analytic, and therefore the false frequencies do not appear.

References

[1] J.M. Maldacena, *The large-N limit of superconformal field theories and supergravity*, *Adv. Theor. Math. Phys.* **2** (1998) 231 [*Int. J. Theor. Phys.* **38** (1999) 1113] [hep-th/9711200];
S.S. Gubser, I.R. Klebanov and A.M. Polyakov, *Gauge theory correlators from non-critical string theory*, *Phys. Lett.* **B 428** (1998) 105 [hep-th/9802109];
E. Witten, *Anti-de Sitter space and holography*, *Adv. Theor. Math. Phys.* **2** (1998) 253 [hep-th/9802150].

[2] S.S. Gubser, I.R. Klebanov and A.W. Peet, *Entropy and temperature of black 3-branes*, *Phys. Rev.* **D 54** (1996) 3915 [hep-th/9602135];
I.R. Klebanov and A.A. Tseytlin, *Entropy of near-extremal black p-branes*, *Nucl. Phys.* **B 475** (1996) 164 [hep-th/9604089];
E. Witten, *Anti-de Sitter space, thermal phase transition and confinement in gauge theories*, *Adv. Theor. Math. Phys.* **2** (1998) 505 [hep-th/9803131].

[3] B. Muller and J.L. Nagle, *Results from the relativistic heavy ion collider*, *Ann. Rev. Nucl. Part. Sci.* **56** (2006) 93 [nucl-th/0602029].

[4] F. Karsch, *Lattice QCD at high temperature and density*, *Lect. Notes Phys.* **583** (2002) 209 [hep-lat/0106019].

[5] G. Policastro, D.T. Son and A.O. Starinets, *The shear viscosity of strongly coupled $N = 4$ supersymmetric Yang-Mills plasma*, *Phys. Rev. Lett.* **87** (2001) 081601 [hep-th/0104066];
P. Kovtun, D.T. Son and A.O. Starinets, *Viscosity in strongly interacting quantum field theories from black hole physics*, *Phys. Rev. Lett.* **94** (2005) 111601 [hep-th/0405231].

JHEP09(2007)057

[6] C.P. Herzog, A. Karch, P. Kovtun, C. Kozcaz and L.G. Yaffe, *Energy loss of a heavy quark moving through $N = 4$ supersymmetric Yang-Mills plasma*, *JHEP* **07** (2006) 013 [hep-th/0605158];
S.S. Gubser, *Drag force in AdS/CFT*, *Phys. Rev.* **D 74** (2006) 126005 [hep-th/0605182];
J. Casalderrey-Solana and D. Teaney, *Heavy quark diffusion in strongly coupled $N = 4$ Yang-Mills*, *Phys. Rev.* **D 74** (2006) 085012 [hep-ph/0605199].

[7] H. Liu, K. Rajagopal and U.A. Wiedemann, *Calculating the jet quenching parameter from AdS/CFT*, *Phys. Rev. Lett.* **97** (2006) 182301 [hep-ph/0605178]; *An AdS/CFT calculation of screening in a hot wind*, *Phys. Rev. Lett.* **98** (2007) 182301 [hep-ph/0607062];
H. Liu, K. Rajagopal and U.A. Wiedemann, *Wilson loops in heavy ion collisions and their calculation in AdS/CFT*, *JHEP* **03** (2007) 066 [hep-ph/0612168];

[8] P.K. Kovtun and A.O. Starinets, *Quasinormal modes and holography*, *Phys. Rev.* **D 72** (2005) 086009 [hep-th/0506184].

[9] K.D. Kokkotas and B.G. Schmidt, *Quasi-normal modes of stars and black holes*, *Living Rev. Rel.* **2** (1999) 2 [gr-qc/9909058];
H. P. Nollert, *Topical review: quasinormal modes: the characteristic 'sound' of black holes and neutron stars*, *Class. and Quant. Grav.* **16** (1999) 159.

[10] G.T. Horowitz and V.E. Hubeny, *Quasinormal modes of AdS black holes and the approach to thermal equilibrium*, *Phys. Rev.* **D 62** (2000) 024027 [hep-th/9909056].

[11] D. Birmingham, I. Sachs and S.N. Solodukhin, *Conformal field theory interpretation of black hole quasi-normal modes*, *Phys. Rev. Lett.* **88** (2002) 151301 [hep-th/0112055].

[12] A.O. Starinets, *Quasinormal modes of near extremal black branes*, *Phys. Rev.* **D 66** (2002) 124013 [hep-th/0207133].

[13] A. Núñez and A.O. Starinets, *AdS/CFT correspondence, quasinormal modes and thermal correlators in $N = 4$ sym*, *Phys. Rev.* **D 67** (2003) 124013 [hep-th/0302026].

[14] V. Cardoso, R. Konoplya and J.P.S. Lemos, *Quasinormal frequencies of Schwarzschild black holes in Anti-de Sitter spacetimes: a complete study on the asymptotic behavior*, *Phys. Rev.* **D 68** (2003) 044024 [gr-qc/0305037].

[15] R.A. Konoplya, *Gravitational quasinormal radiation of higher-dimensional black holes*, *Phys. Rev.* **D 68** (2003) 124017 [hep-th/0309030].

[16] N. Andersson and K.E. Thylwe, *Complex angular momentum approach to black hole scattering*, *Class. and Quant. Grav.* **11** (1994) 2991.

[17] C. Csáki, H. Ooguri, Y. Oz and J. Terning, *Glueball mass spectrum from supergravity*, *JHEP* **01** (1999) 017 [hep-th/9806021].

[18] R. de Mello Koch, A. Jevicki, M. Mihailescu and J.P. Nunes, *Evaluation of glueball masses from supergravity*, *Phys. Rev.* **D 58** (1998) 105009 [hep-th/9806125].

[19] R.C. Brower, S.D. Mathur and C.-I. Tan, *Glueball spectrum for QCD from AdS supergravity duality*, *Nucl. Phys.* **B 587** (2000) 249 [hep-th/0003115].

[20] D. Bak, A. Karch and L.G. Yaffe, *Debye screening in strongly coupled $N = 4$ supersymmetric Yang-Mills plasma*, arXiv:0705.0994.

[21] S.A. Hartnoll and S. Prem Kumar, *AdS black holes and thermal Yang-Mills correlators*, *JHEP* **12** (2005) 036 [hep-th/0508092].

JHEP09(2007)057

[22] D.T. Son and A.O. Starinets, *Minkowski-space correlators in AdS/CFT correspondence: recipe and applications*, *JHEP* **09** (2002) 042 [hep-th/0205051].

[23] H. Kodama and A. Ishibashi, *A master equation for gravitational perturbations of maximally symmetric black holes in higher dimensions*, *Prog. Theor. Phys.* **110** (2003) 701 [hep-th/0305147].

[24] V. Cardoso, J. Natario and R. Schiappa, *Asymptotic quasinormal frequencies for black holes in non-asymptotically flat spacetimes*, *J. Math. Phys.* **45** (2004) 4698 [hep-th/0403132]; J. Natario and R. Schiappa, *On the classification of asymptotic quasinormal frequencies for D-dimensional black holes and quantum gravity*, *Adv. Theor. Math. Phys.* **8** (2004) 1001 [hep-th/0411267].

[25] G. Policastro, D.T. Son and A.O. Starinets, *From AdS/CFT correspondence to hydrodynamics*, *JHEP* **09** (2002) 043 [hep-th/0205052].

[26] G. Policastro, D.T. Son and A.O. Starinets, *From AdS/CFT correspondence to hydrodynamics. II: sound waves*, *JHEP* **12** (2002) 054 [hep-th/0210220].

[27] E.W. Leaver, *An analytic representation for the quasi normal modes of Kerr black holes*, *Proc. Roy. Soc. Lond.* **A 403** (1985) 285.

[28] C. Hoyos, K. Landsteiner and S. Montero, *Holographic meson melting*, *JHEP* **04** (2007) 031 [hep-th/0612169].

[29] R.C. Myers, A.O. Starinets and R.M. Thomson, *Holographic spectral functions and diffusion constants for fundamental matter*, arXiv:0706.0162.

[30] R.S. Maier, *The* 192 *Solutions of the Heun equation*, *Math. Comp.* **76** (2007) 811 [math.CA/0408317].

[31] P. Breitenlohner and D.Z. Freedman, *Positive energy in Anti-de Sitter backgrounds and gauged extended supergravity*, *Phys. Lett.* **B 115** (1982) 197.

[32] A. Ishibashi and H. Kodama, *Stability of higher-dimensional Schwarzschild black holes*, *Prog. Theor. Phys.* **110** (2003) 901 [hep-th/0305185].

[33] V. Cardoso and J.P.S. Lemos, *Quasi-normal modes of Schwarzschild Anti-de Sitter black holes: electromagnetic and gravitational perturbations*, *Phys. Rev.* **D 64** (2001) 084017 [gr-qc/0105103].

[34] E. Berti and K.D. Kokkotas, *Quasinormal modes of Reissner-Nordstroem-Anti-de Sitter black holes: scalar, electromagnetic and gravitational perturbations*, *Phys. Rev.* **D 67** (2003) 064020 [gr-qc/0301052].

JHEP09(2007)057